

Dielectric response of HBr condensed into mesoporous glass

D. Wallacher,¹ T. Hofmann,¹ K. Knorr,¹ and A. V. Kityk²

¹*Technische Physik, Universität des Saarlandes, 66041 Saarbrücken, Germany*

²*Institute for Computer Science, Technical University of Czestochowa, Electrical Engineering Department, Al. Armii Krajowej 17, PL-42200 Czestochowa, Poland*

(Received 31 January 2005; published 13 June 2005)

HBr gas has been condensed into mesoporous glasses and solidified by cooling. The pore filling has been investigated by broad band permittivity measurements and x-ray diffraction. The pore confined material basically reproduces the phase sequence of the bulk system (liquid-cubic-orthorhombic), but the phase transition temperatures are strongly reduced. Special attention has been paid to the paraelectric-ferroelectric transition within the orthorhombic regime. The dielectric dispersion allows to discriminate between the material next to the pore walls and the capillary condensed fraction in the pore centers.

DOI: 10.1103/PhysRevB.71.224202

PACS number(s): 61.43.Gt, 61.43.Fs, 64.70.Nd, 77.22.-d

I. INTRODUCTION

The confinement in mesopores affects the relaxational behavior of molecular liquids. Appropriate experimental methods are quasielastic neutron scattering and broadband dielectric spectroscopy. Particular interest has been paid to glass forming liquids such as glycerol in various types of mesoporous silica.¹⁻⁵ The observed shift of the glass transition temperature has been taken as an indication that this transition is very much like a second-order phase transition-subject to finite size effects, which in turn means that there is a coherence length connected with the glass transition.² Another series of experiments, on smaller molecules, has shown that the observed changes with respect to the bulk state are by no means simply due to the geometric confinement, but to the interactions of the filling with the pore walls. Already adsorption isotherms demonstrate in a convincing way that due to the strong attractive substrate potential the first fractions of vapor that condense in the pores form an adsorbed film on the pore walls.^{6,7} Only thereafter the pores are filled by capillary condensation. The adsorbed film is different from the capillary condensate. This is particularly obvious in the solid regime. The capillary condensate is basically bulklike, with a crystal structure that is close if not identical to that of the bulk system. It usually reproduces the phase transitions of the bulk system. The adsorbed film, however, is amorphous, it mimics the amorphous state of the silica substrate, and does not participate in the phase transitions. The main difference between the capillary condensed fraction and the bulk state are the downshifts ΔT_s of the transition temperatures T_s and the thermal hysteresis of the transitions. Most pertinent information exists on the melting/freezing transition, but there also data on structural phase transitions, e.g., for O₂ and CO in Vycor glass.^{7,8} The transitions studied so far are all of first order. Here the shift of the transition temperature relative to the bulk system can be explained in terms of a competition of interfacial and volume free energies.⁹

Our previous studies on the dielectric properties of small molecules embedded in mesoporous glasses dealt with Ar, CO,¹⁰ and CH₃CN.¹¹ These studies have shown that the adsorbed film on the pore walls and the capillary condensed fraction of the pore filling have different dielectric proper-

ties. Attempts have been made to isolate the response of the pore filling from the effective permittivity of the composite and to identify the contributions of the terminal OH groups of the silica matrix. For CO the main interest was in the freezing of head-tail flips of the molecules. The study on acetonitrile concentrated on the dielectric behavior at the freezing transition and at a subsequent first-order structural transition between two electrically ordered phases.

In the present article we pose the question of how pore confinement affects a second-order phase transition. The system chosen is HBr in porous Vycor glass. This substrate has an average pore diameter of about 7 nm, which is equivalent to 17 intermolecular distances. At first glance HBr appears to be an ideal choice. It is presumably the simplest ferroelectric material from a crystallographic point of view. The paraferro-transition is of second order, or at least nearly so. The triple point is well below room temperature. This allows the measurement of adsorption isotherms on this polar molecule with the cryogenic equipment at hand in our laboratory, which in turn means that partial fillings can be prepared in a controlled way in order to discriminate between the adsorbed film and the quasibulk capillary condensate. On the other hand, information on bulk HBr is scarce; it mainly dates from the early days of ferroelectricity. This is due to problems related to the handling of this substance. HBr is chemically aggressive, solid samples have to be prepared in situ in cryogenic equipment, the contraction of the samples on cooling produces cracks, a serious problem in permittivity studies, the texture of polycrystalline or the orientation of single crystalline samples is usually unknown. For these reasons HBr has not developed into a model (order-disorder-type) ferroelectric.

Bulk HBr solidifies at 186.3 K into the cubic phase I (fcc, $Fm\bar{3}m$) in which the HBr dipoles reorient rapidly between 12 equivalent crystallographic directions. The transition at 116.9 K takes the system into the cubic phase I' ($Pa\bar{3}$) in which the H atom reorients in a plane formed by 6 out of the 12 nearest neighbor Br atoms. Below 113.6 K the bulk system is orthorhombic with a transition at $T_c = 89.7$ K from the paraelectric phase II ($Bbcm$) with two equivalent positions of the H atom into the completely ordered phase III ($Bb2_1m$).^{12,13} In par-

ticular in the orthorhombic phases the H atom points to a Br next neighbor, suggesting directional Br-H \cdots Br bonds. The relevance of H bonds is supported by the value of the spontaneous polarization P_s (Ref. 14) that is lower than expected for free HBr dipoles, the anomalous frequencies of the H-Br stretching modes and by MD simulations.¹⁵ Phase III actually has a canted antiferroelectric structure with a zig-zag line of HBr molecules propagating along the b direction which is also the direction of the spontaneous polarization P_s . P-E hysteresis loops demonstrate ferroelectric switching.¹⁴ Measurements of the permittivity (ϵ) show strong dispersion in the orthorhombic phases with one dispersion branch in phase II that shows some slowing down when approaching T_c from above and two branches in phase III. The two branches may be related to the elements of the ϵ tensor parallel and perpendicular to P_s , alternatively it has been suggested that the lower branch refers to domain wall motion. The static permittivity ϵ_{st} of polycrystalline samples as obtained from extrapolations of the (skewed) arcs of complex plane plots to zero frequency, shows maximum values of ϵ_{st} right at T_c . The actual values vary strongly from sample to sample, presumably because of cracks or different textures of the samples. For the most favorable case reported in the literature, $\epsilon_{st}(T)$ shows a sharp maximum at T_c with $\epsilon_{st}=200$ (Ref. 16), which in fact suggests that ϵ_b , the critical component of the ϵ tensor, indeed diverges at T_c , as one expects for a second-order ferroelectric phase transition. Unfortunately there are no permittivity experiments on single crystals that could have given direct access to this component. The λ shape of the heat capacity,¹⁷ the slowing down of the dielectric relaxations¹⁸ and the crystallographic group-subgroup relation between phase II and III are further arguments in favor of a continuous transition.

II. EXPERIMENTAL

The porous matrix for the permittivity measurements is a slab of Vycor glass (code 7930, Corning) with a thickness d of 0.23 mm. The porosity is 0.30 and the average pore diameter 7 nm. Evaporated Au films with an area A of 50 mm² serve as electrodes for the permittivity measurements. The geometric capacitance $C_g = \epsilon_0 A/d$ is (1.9 ± 0.05) pF. The sample is inserted in a cell that is bolted to the cold plate of a closed cycle He refrigerator. HBr gas has been admitted in volumetrically controlled portions via a heated capillary that connects the cell with a gas handling system that is equipped with a membrane pressure gauge. We tried to record a complete adsorption isotherm at 175 K, but encountered the problem that the pressure after admitting a new dose of gas never really equilibrated. The reason for this failure became clear at the end of the experiments. The gas leading parts showed traces of corrosion (the pumps even had to be replaced), the gas obviously reacted with the metal surfaces. The values quoted for the fractional fillings $f=0.32, 0.49, 0.66$, are therefore only rough estimates, accurate to ± 0.05 , that are based on the volumetric data in combination with the permittivity data interpolated between $f=0$ and $f=1$. The onset of capillary condensation is at about $f=0.5$. In order to guarantee complete filling, $f=1$, the Vycor matrix was in fact

heavily overfilled; the excess condensate outside the pores has no effect on the measured permittivity. The dielectric data $C = \text{Re } C + i \text{Im } C = C_g(\epsilon' + i\epsilon'')$ have been collected at 30 different frequencies $\omega/2\pi$ ranging from 0.1 Hz to 1 MHz with an impedance analyzer in combination with an impedance matching interface (Solartron SI-1255 and SI-1296). X-ray diffraction patterns (intensity I as a function of the scattering angle 2θ) have been recorded in a similar setup in a cell equipped with Be windows. Coupled 2θ - θ scans have been used. The wavelength was 1.542 Å (CuK $_{\alpha}$). Here a controlled pore glass (Gelsil) was used as a substrate that has about the same pore diameter but a higher porosity. Therefore the intensity ratio of the Bragg peaks of the solidified pore filling with respect to the glass background is more favorable than for Vycor. Studies on Ar in Vycor and Gelsil⁶ have shown that there is little difference between these two substrates as long as the pore diameters are identical. The diffraction experiments have been carried out for an almost completely filled sample.

III. RESULTS AND DISCUSSION

The diffraction patterns as observed on cooling down from 175 K to 25 K and back up to 175 K in steps of 5 K are shown in Fig. 1. The background as obtained on an empty sample has been subtracted. At the highest temperatures the pore filling is liquid as evidenced by the smooth variation of the scattered intensity as function of 2θ . The first two maxima of the structure factor of the liquid state can be identified. The Bragg peaks of the solid appear on cooling at $T_f=145$ K. On heating they persist up to $T_m=165$ K. The freezing/melting temperature T_m^{bulk} of the bulk system is 186.3 K. The relative shift with respect to the bulk state and the relative width of the thermal hysteresis of the liquid-solid transition are quite similar to what has been observed for Ar in pores with the same size.⁶ After solidification the structure of the pore filling is fcc, as for the bulk state. The fcc peaks observed are (111), (200), (220), (311), and (222), listed with increasing 2θ . The (222) reflection shows up as the weak feature at $2\theta=55^\circ$. The lattice constant is 5.81 Å, which is within the error of the experiment identical with that of the bulk system. The intrinsic peak width Δ (in units of $\sin \theta$) is independent of the node index, suggesting finite size L broadening, with L of the order of 100 nm. This value is much larger than the pore diameter, obviously the coherence of the lattice extends over quite long distances along the pore axes. The (200) peak that is sensitive to stacking faults is well resolved. The stacking fault probability α is lower than for the best examples of diffraction patterns on pore condensed fcc Ar.⁶ The upper estimate for α is 3%. Obviously the directional bonding of HBr reduces the number of stacking faults relative to Ar. The x-ray Bragg intensities stem from the Br atoms, are practically insensitive to the H-positions and hence to the dipolar degrees of freedom. For this reason the diffraction experiment cannot distinguish between the phases I and I' and between the phases II and III. Thus there is, e.g., no chance of detecting the (210) reflection that would discriminate phase I from phase I'. Since furthermore the change of the lattice parameters expected for the I-

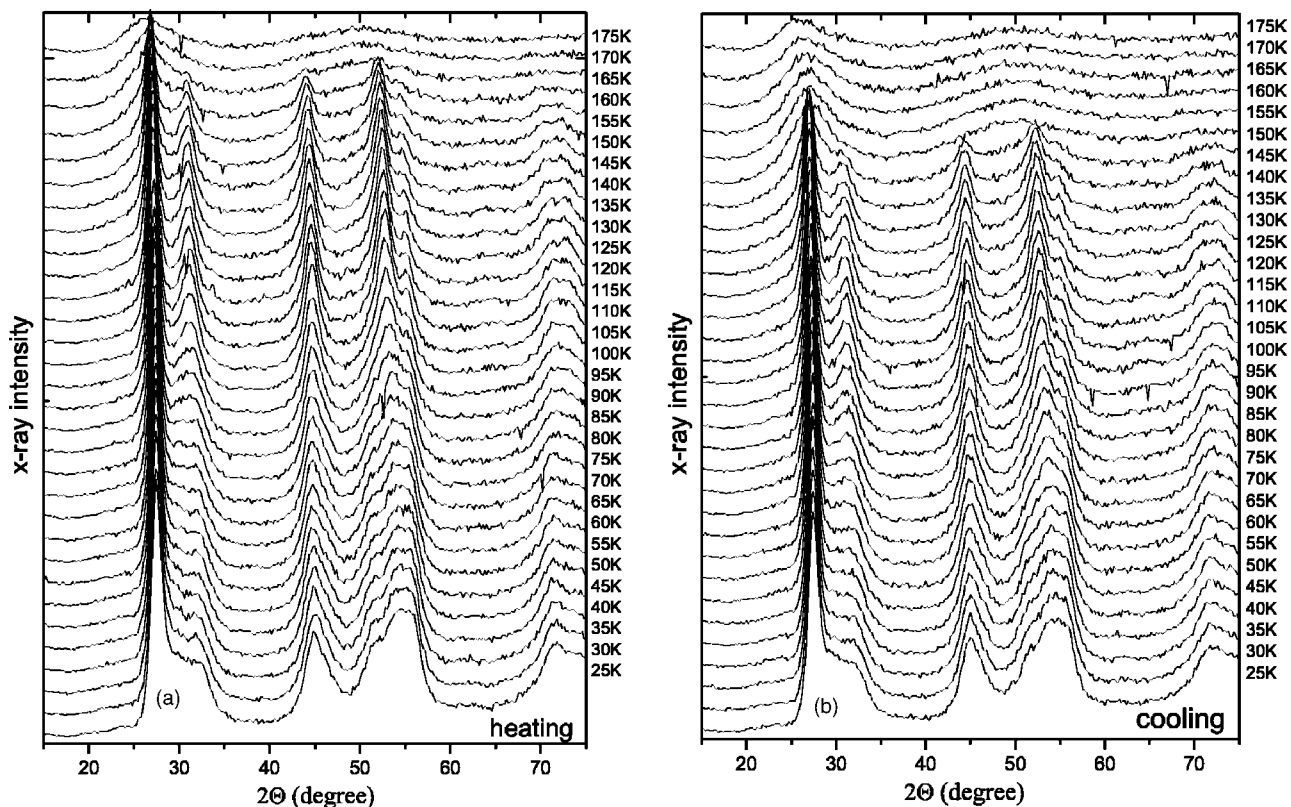


FIG. 1. Powder diffraction patterns of HBr in Vycor ($f \approx 1$) as obtained on heating (a) and cooling (b).

I' and for the II-III transition is small compared to the finite size broadened peak width, the diffraction experiment cannot give information on these transitions. In fact it is even difficult to localize the cubic-orthorhombic transition (I or I') to (II or III) in the data of Fig. 1. The uniaxial components δ_{aa} , δ_{bb} , δ_{cc} of the spontaneous strain tensor at this transition should lead to peak splittings that are in principle large enough to be observed in the present experiment. The results of Fig. 1 fail to show such splittings but do show a gradual broadening of the (200) and the (311) peak that are most susceptible to such strains. These changes extend over about 25 K and are centered at 65 K on cooling and at 85 K on heating. There is no effect on the (111) peak, suggesting that there is no spontaneous shear deformation, in agreement with the situation in the bulk system. The bulk transition temperature is 113.6 K. Thus there is a dramatic relative downshift of this transition. Altogether these observations suggest a wide distribution of the transition temperature and of the spontaneous strain order parameter, cubic-orthorhombic phase coexistence, and metastable states.

The patterns of the solid state also contain a background from an amorphous component, which is presumably related to the pore condensate next to the pore walls. The volume fraction of this component is difficult to estimate, having just data on $f \approx 1$ at hand.

Figure 2 shows the T dependence of $Re C$ and $Im C$ for some selected frequencies, as recorded on cooling down a sample with $f=1$. In the liquid state and at low frequencies, $Re C$ and $Im C$ are extremely large. This behavior could be due to Maxwell-Wagner-Sillars,¹⁹ to dc or hopping

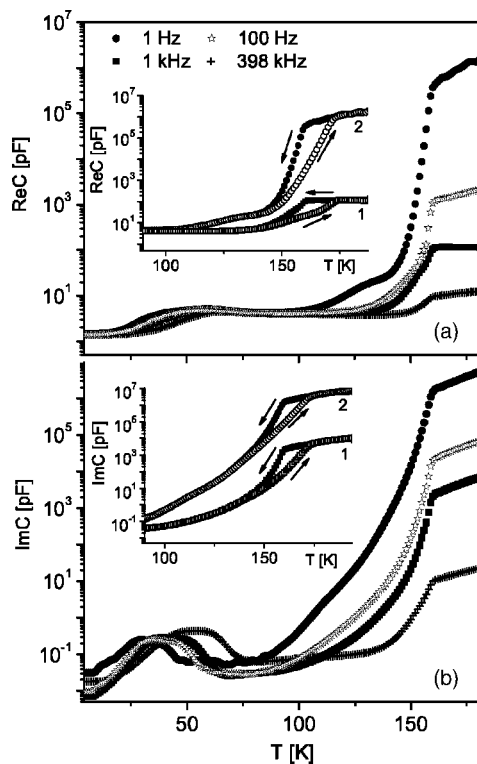


FIG. 2. $Re C$ (a) and $Im C$ (b) versus the temperature of HBr condensed into nanopores ($f=1.0$) recorded on cooling for several frequencies. The insets show the thermal hysteresis in the region of liquid-solid coexistence. Curves labeled 1 are 1 kHz data, curves labeled 2 are 1 Hz data.

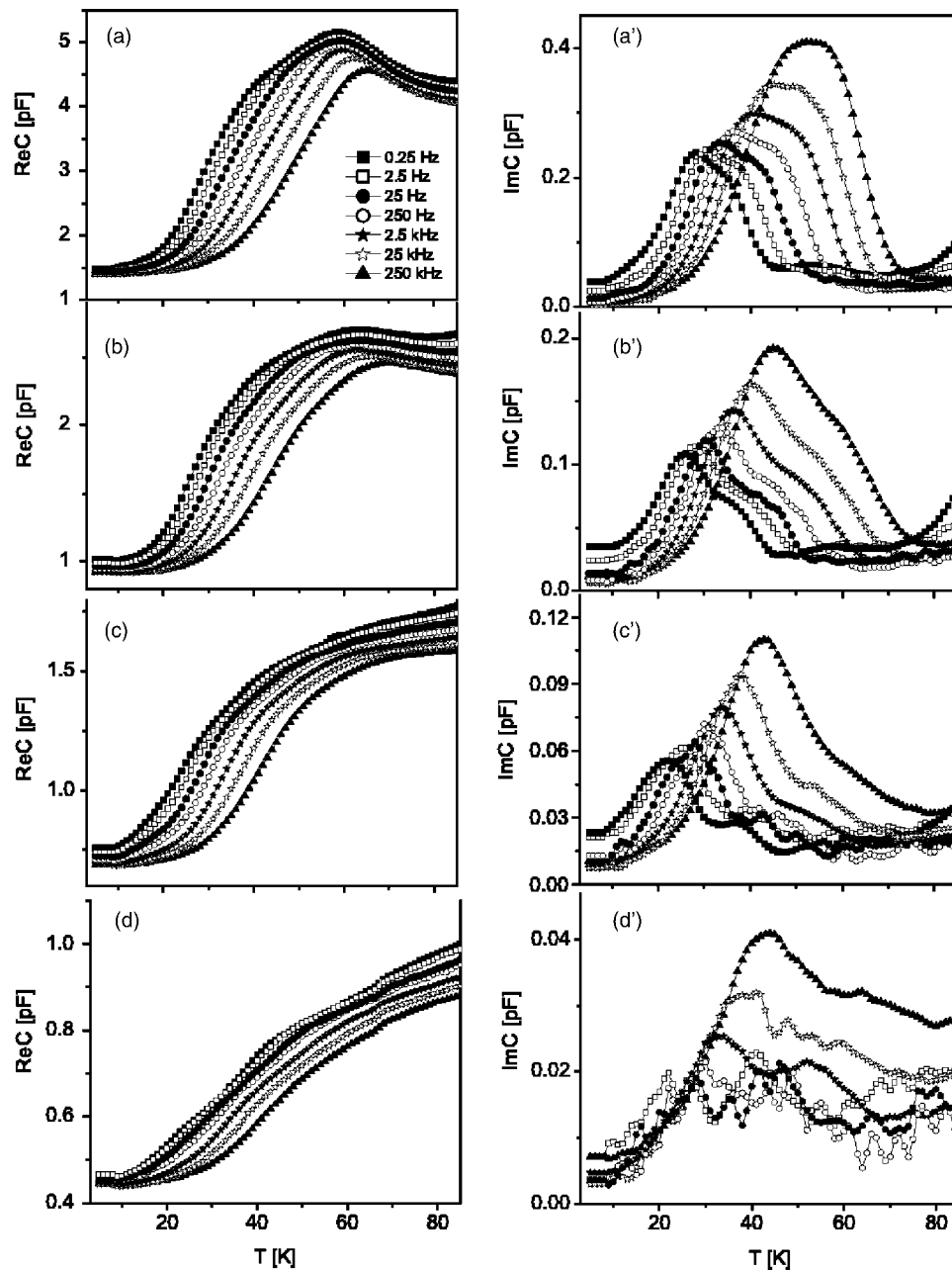


FIG. 3. Temperature dependencies of $\text{Re } C$ (a-d) and $\text{Im } C$ (a'-d') as obtained on cooling for several frequencies and fractional fillings: $f=1.0$ (a, a'), $f=0.66$ (b, b'), $f=0.49$ (c, c') and $f=0.32$ (a, a'). The “background” real and imaginary capacity of glass matrix is subtracted.

conductivity.²⁰ The onset of solidification (at $T_f=155$ K) as well as the termination of the melting process (at $T_m=170$ K) is signaled by a kink of the data curves of Fig. 2. These features are independent of the measuring frequency, as is expected for a first-order phase transition. The values of the freezing and melting temperature roughly agree with those derived from the diffraction measurement. Residual discrepancies between the permittivity and the diffraction experiment are due to the finite T steps and the detection limit of the minority phase of the diffraction experiment, but perhaps also to a slight difference of the pore diameter of the Vycor and the Gelsil matrix. The change of the permittivity on solidification and melting are by no means steplike, as observed for the bulk system, but there is a rather gradual

frequency-dependent drop of the dielectric response toward low T . For the lowest frequencies it extends down to below 100 K. The main part of this decrease is due to a gradual transformation of the liquid into a solid. This process is completed at about 140 K, the lower closing point of the heating-cooling hysteresis of the permittivity curves (inset of Fig. 2). Altogether the freezing/melting process of HBr appears to be quite similar to that of other pore fillings in the disordered pore network of Vycor and similar substrates. The downshift of the transition, the wide range of phase coexistence, as well as the sharp onset of freezing and the sharp termination of melting have been explained by simple thermodynamic that is based on the idea of a radial arrangement of the coexisting phases in combination with a pore size distribution.⁹ The

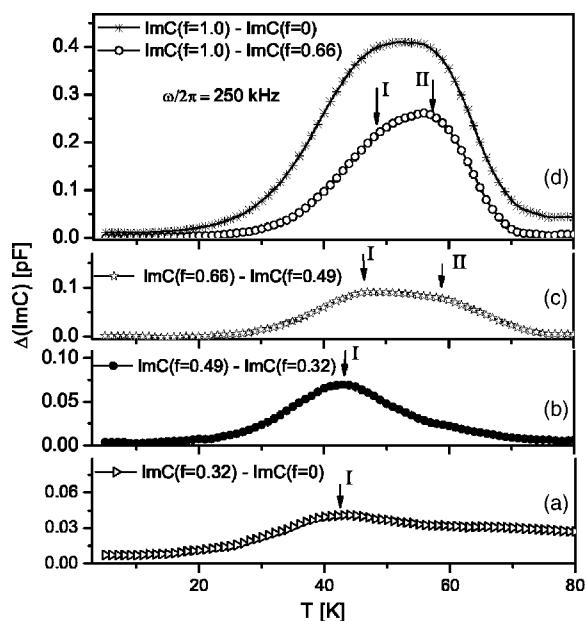


FIG. 4. The T dependence of the difference of $\text{Im } C$ (measured at $\omega/2\pi=250$ kHz) of samples with different degrees of pore filling. The panels a, b, c, d represent the first two monolayers, the third monolayer, a small amount, and the maximum amount of capillary condensate, respectively.

permittivity continues to decrease below 140 K. This is likely to be due to a gradual freezing of the reorientations of the HBr dipoles within the cubic (I or I') regime. Unfortunately there are no clear fingerprints such as a ω -dependent dispersion step of $\text{Re } C$ and a maximum of $\text{Im } C$ (other than a shoulder observable at low ω) that would allow the extraction of the relaxation parameters of this process.

Our attention concentrates on the low- T regime from 5 K to 90 K in which we search for effects that are related to ferroelectric ordering. The dielectric dispersion observed here is very broad and leaves the experimental ω window at higher T . Traces of $\text{Re } C$ and $\text{Im } C$ as a function of T are shown in Fig. 3 for a number of frequencies and different filling fractions. The contribution of the glass matrix, as obtained from a measurement on the empty matrix, has been subtracted. As far as the different filling levels are concerned we assume, guided by the volumetric adsorption data on the present sample and by various types of data on other pore fillings,^{6-8,10} that the samples with $f=0.32$ and 0.49 have just an amorphous HBr film adsorbed on the pore walls and that it is only beyond f about 0.5, that is for the samples with $f=0.66$ and 1 , that the pore centers are progressively filled with the capillary condensate. We expect that the capillary condensed fraction shows quasibulk behavior, but that the adsorbed film on the pore walls does not. The changes of the dielectric response with f are apparent from Fig. 3. For low f , that is for HBr films adsorbed on the pore walls, there is a broad dispersion step of $\text{Re } C$ and a corresponding maximum of $\text{Im } C$ with a long tail toward high T . For the samples containing a capillary condensate, that is for $f=0.66$ but in particular for $f=1$, there is an additional contribution at temperatures around 60 K. In Fig. 4 the 250 kHz data are replotted, taking the difference of $\text{Im } C$ between neighboring val-

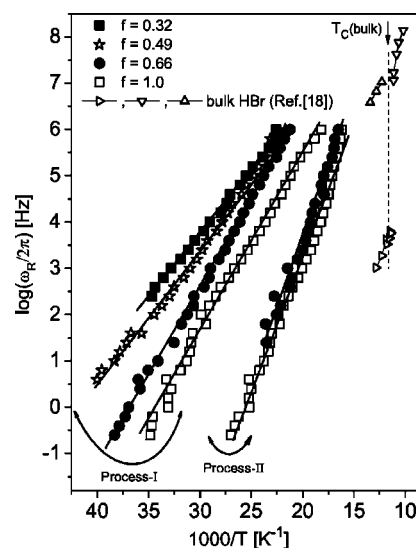


FIG. 5. Relaxation frequency versus $1/T$ for the glass matrix filled with HBr. The filling fractions are indicated. The pre-exponential factor and the energy barrier of the Arrhenius law are as follows: Process I: $\tau_{10}=(1.12\pm 0.15)\times 10^{-13}$ s, $E_{10}=1290\pm 20$ cal/mol ($f=0.32$); $\tau_{10}=(5.6\pm 0.5)\times 10^{-14}$ s, $E_{10}=1385\pm 20$ cal/mol ($f=0.49$); $\tau_{10}=(8.9\pm 0.9)\times 10^{-16}$ s, $E_{10}=1765\pm 30$ cal/mol ($f=0.66$); $\tau_{10}=(5.0\pm 0.5)\times 10^{-15}$ s, $E_{10}=1795\pm 30$ cal/mol ($f=1.0$); Process II: $\tau_{20}=(2.1\pm 0.6)\times 10^{-17}$ s, $E_{20}=2815\pm 60$ cal/mol ($f=0.66$); $\tau_{20}=(2.6\pm 0.5)\times 10^{-16}$ s, $E_{20}=2660\pm 40$ cal/mol ($f=1.0$).

ues of f . This figure suggests that there are two relaxations, labeled I and II. Process I is borne by the film, and in fact there is little change when increasing the thickness from $f=0.32$, equivalent to about two monolayers, to $f=0.49$, equivalent to about three monolayers adsorbed on the pore walls. Nevertheless the maximum of $\text{Im } C$, which is at 42 K for $\omega/2\pi=250$ kHz, is sharper for the third monolayer than for the first two. Obviously the distribution of relaxation rates is particularly wide for HBr molecules in direct contact with the pore walls, as is likely considering the heterogeneous character of the substrate. For the third layer the influence substrate potential on the HBr dynamics is already reduced, and accordingly the distribution of relaxation rates is narrower than for the first two monolayers. Process II is due to the capillary condensate. Both relaxations are thermally activated, as is documented in the Arrhenius plot of Fig. 5.

Process II is the slower one, relaxations of this type have to overcome higher barriers. This appears plausible, considering the fact that the capillary condensate is well crystallized. The barrier of process I increases somewhat with increasing f , suggesting that even for the amorphous film on the pore walls the structural order increases with the distance from the glass substrate. Process II roughly extrapolates the fast dispersion branch of the bulk system¹⁸ (Fig. 5).

At least for the lower frequencies, the T position of the maximum of $\text{Re } C$ around 60 K for the two samples that contain some capillary condensate is independent of ω (Fig. 3, frames a and b). This is consistent with a phase transition. In order to extract the static limit of the capacitance, C_{st} , the dielectric data for $f=1$ are shown in a complex-plane plot

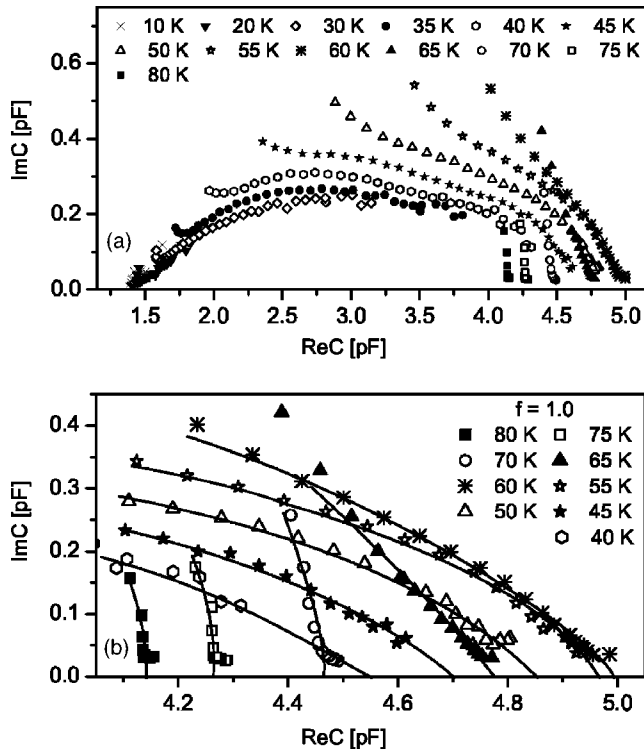


FIG. 6. Cole-Cole plot of the glass matrix completely filled with HBr, panel a. Panel b shows the right wing of the arcs in more detail. The solid lines extrapolate to the static value on the real axis.

(Fig. 6). The resulting traces are sections of arcs that deviate significantly from a circular shape, due to the overlap of the two relaxational channels. For a T interval from about 40 K to 80 K the static limit of C can be extracted in a reliable way. The results are shown in Fig. 7. For $f=1$, C_{st} shows a maximum centered at 58 K. Remainders of this maximum can be identified also for $f=0.66$, but this feature is absent for the lower two filling fractions for which there is no capillary condensate present. We relate the maximum to a phase transition at $T_c=58$ K of the capillary condensate and think of the ferroelectric II-III transition.

The relative shift Δt of T_c with respect to the bulk system is 0.35. In a finite sample, the sample size L sets a limit to the coherence length of the critical fluctuations of a second-order phase transition. This leads to a shift of the apparent transition temperature relative to the infinite bulk system obeying the scaling relation $\Delta t=A(1/L)^{1/\nu}$, ν is the critical exponent of the correlation length. Identifying L with the pore diameter, equivalent to 17 intermolecular distances, and choosing the ν value of the 3D Ising class ($=0.64$), the observed T_c reduction calls for a value of about 30 for the nonuniversal coefficient A . This value is much higher compared to what is usually obtained in computer studies of phase transitions,²² even if the relevant interactions are of short range. This suggests that the reduction of T_c is not just a matter of the finite size, but is also due to the substrate potential acting on the capillary condensate. In particular we think of the effects of “clamping.” The onset of the spontaneous ferroelectric polarization at T_c is accompanied by spontaneous strains. The strains of phase III well below T_c with respect to phase II are

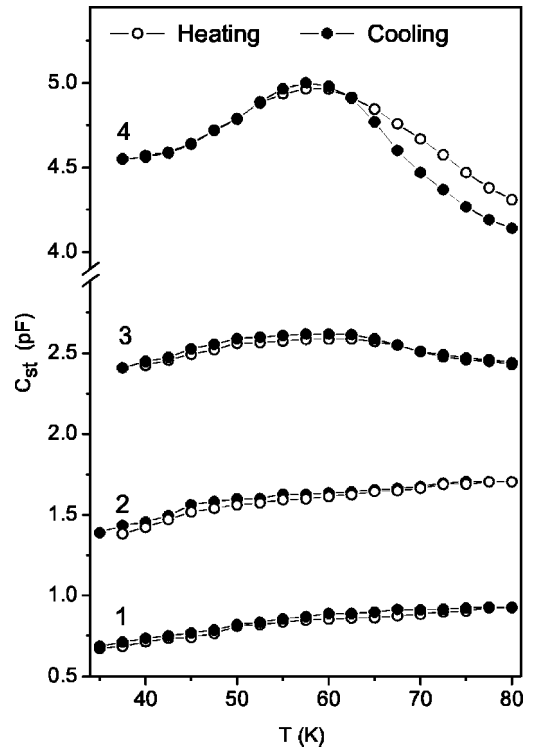


FIG. 7. Static capacitance versus the temperature of HBr condensed into nanopores: $f=0.32$ (1), $f=0.49$ (2), $f=0.66$ (3), and $f=1.0$ (4). The background of the empty glass matrix has been subtracted.

of the order of 1%. This is not much, but nevertheless the blocking of such strains in confinement delays ferroelectric ordering.

In the following the ratio R of the static permittivity ϵ_{eff} of the silica-HBr composite at T_c and well away from T_c , say at $T=T_c \pm 20$ K, is discussed. R is a measure of to what extent the dielectric response “diverges” at T_c . Using the $f=1$ data of Fig. 7 and adding the capacity of the empty matrix of 5.3 pF, gives $R=1.07$. Can this rather modest value be compatible with a divergence of ϵ_b at a ferroelectric phase transition of second order? Simple expressions of ϵ_{eff} as a function of the permittivities and volume fractions of the components are only available for highly idealized cases, such as, e.g., isolated spherical or ellipsoidal inclusions of one medium in a host medium. Clearly these assumptions are not fulfilled; the pores form a continuous network. Calculations based on the method of finite elements, a questionable approach given the nm-scale partition of the samples, would require knowledge of the topology of pore space and of the orientation of the ϵ tensor of orthorhombic HBr in the pore segments. The information available is restricted to the porosity and the average pore diameter. We estimate R based on the best permittivity data available on the bulk sample,¹⁶ with $\epsilon(T_c)=200$, $\epsilon(T_c \pm 20 \text{ K}) \approx 30$. A lower bound for the R value of the composite is obtained by assuming that the composite consists of a layer of SiO_2 and a layer of HBr in series with the relative thicknesses $(1-P_{eff})$ and P_{eff} , respectively. P_{eff} is about 0.2, somewhat smaller than the nominal porosity of 0.29, since the ferroelectric response is only due to the cap-

illary condensed fraction of the pore filling. This estimate gives $R=1.03$. With the same entries the Hanai-Bruggeman formula for randomly arranged spherical inclusions interacting via dipole fields gives $R=1.33$, see e.g., Refs. 20 and 21 for this and other expressions for the permittivity of a composite. These estimates show that the incomplete filling of the space between the electrodes with the active medium has a devastating effect on the ferroelectric response at T_c . The permittivity is furthermore subject to finite size effects, $\epsilon(T_c) \propto L^{\gamma/\nu}$, γ is the critical exponent of the susceptibility (1.38 for the 3D Ising model). Thus the low R value observed is not in contradiction with a second-order phase transition of the HBr pore filling. The absence of thermal hysteresis is an argument in favor of the continuous character of this transition.

The static dielectric response of the $f=1$ sample shows hysteresis with respect to heating and cooling extending from about 65 K to temperatures above 80 K (Fig. 7). Guided by the x-ray results we suggest that this is due to the cubic-orthorhombic transition. The I'-II transition is of first order and shows a slight thermal hysteresis already in the bulk state.¹⁶ The downshift of the transition temperature and the relatively broad T interval of phase coexistence can be explained qualitatively in terms analogous to what has been cited for the liquid-solid transition, namely a competition of the volume free energy and the cubic-orthorhombic interfacial energy.

IV. CONCLUSION

Our experiments combining diffraction and permittivity measurements have shown that capillary condensed fraction of HBr fillings in the 7 nm pores of Vycor glass crystallizes in the fcc structure and transforms into an orthorhombic structure at lower temperatures. Within the orthorhombic regime there is evidence for a ferroelectric transition. Thus this fraction of the pore filling basically reproduces the phase sequence of the bulk system. The temperatures of the liquid-solid, of the cubic-orthorhombic, and of the ferroelectric transition are shifted to lower temperatures, with relative shifts of up to 45%. In contrast to the two other transitions, the ferroelectric transition does not show thermal hysteresis and the variations of the permittivity, though small, are compatible with a transition of second order in confinement. The material next to the pore walls does not participate in the transitions and shows dielectric dispersion different from the capillary condensed fraction.

ACKNOWLEDGMENT

This work has been supported by the Deutsche Forschungsgemeinschaft (Sonderforschungsbereich 277 "Grenzflächenbestimmte Materialien", Saarbrücken).

-
- ¹D. Daoukaki, G. Barut, R. Pelster, G. Nitz, A. Kyritsis, and P. Pissis, *Phys. Rev. B* **58**, 5336 (1988).
- ²M. Arndt, R. Stannarius, H. Groothues, E. Hempel, and F. Kremer, *Phys. Rev. Lett.* **79**, 2077 (1997).
- ³J. Schüller, R. Richert, and E. W. Fischer, *Phys. Rev. B* **52**, 15232 (1995).
- ⁴M. Arndt, R. Stannarius, W. Gorbatschow, and F. Kremer, *Phys. Rev. E* **54**, 5377 (1996).
- ⁵J. Schüller, Yu. B. Mel'nichenko, R. Richert, and E. W. Fischer, *Phys. Rev. Lett.* **73**, 2224 (1994).
- ⁶P. Huber and K. Knorr, *Phys. Rev. B* **60**, 12657 (1999).
- ⁷P. Huber, D. Wallacher and K. Knorr, *Phys. Rev. B* **60**, 12666 (1999).
- ⁸D. Wallacher, R. Ackermann, P. Huber, M. Enderle, and K. Knorr, *Phys. Rev. B* **64**, 184203 (2001).
- ⁹D. Wallacher and K. Knorr, *Phys. Rev. B* **63**, 104202 (2001).
- ¹⁰D. Wallacher, V. P. Soprunyuk, A. V. Kityk, and K. Knorr, *Phys. Rev. B* **66**, 014203 (2002).
- ¹¹D. Wallacher, V. P. Soprunyuk, K. Knorr, and A. V. Kityk, *Phys. Rev. B* **69**, 134207 (2004).
- ¹²J. K. Cockcroft, A. Simon, and K. R. A. Ziebeck, *Z. Kristallogr.* **184**, 229 (1988).
- ¹³A. Simon, *Z. Naturforsch.* **25b**, 1489 (1970).
- ¹⁴S. Hoshino, K. Shimaoka, and N. Niimura, *Phys. Rev. Lett.* **19**, 1286 (1967).
- ¹⁵T. Ikeda, M. Sprik, K. Terakura, and M. Parinello, *J. Chem. Phys.* **111**, 1595 (1999).
- ¹⁶N. L. Brown and R. H. Cole, *J. Chem. Phys.* **21**, 1920 (1953).
- ¹⁷W. F. Giauque and R. Wiebe, *J. Am. Chem. Soc.* **50**, 2193 (1928).
- ¹⁸P. P. M. Groenewegen and R. H. Cole, *J. Chem. Phys.* **46**, 1069 (1967).
- ¹⁹K. W. Wagner, *Explanation of the Dielectric Fatigue Phenomenon on the Basis of Maxwell's Concept*, *Arkiv für Electrotechnik*, edited by H. Shering (Springer-Verlag, Berlin, 1914).
- ²⁰E. Tuncer, Y. V. Serdyuk, and S. M. Gubanski, *IEEE Trans. Dielectr. Electr. Insul.* **9**, 809 (2002).
- ²¹R. Pelster, *Phys. Rev. B* **59**, 9214 (1999).
- ²²M. E. J. Newman and G. T. Barkenna, *Monte Carlo Methods in Statistical Physics* (Oxford University Press, New York, 1999).